

Stability regions around the components of the triple system 2001 SN263

R. A. N. Araujo,^{1,2★} O. C. Winter,^{1,2★} A. F. B. A. Prado^{1★} and A. Sukhanov^{1★}

¹INPE - National Institute for Space Research, CEP 12201-970, São José dos Campos, SP, Brazil

²UNESP - São Paulo State University, CEP 12516-410, Guaratinguetá, SP, Brazil

Accepted 2012 April 4. Received 2012 April 3; in original form 2012 January 9

ABSTRACT

Space missions are an excellent way to increase our knowledge of asteroids. Near-Earth asteroids (NEAs) are good targets for such missions, as they periodically approach the orbit of the Earth. Thus, an increasing number of missions to NEAs are being planned worldwide. Recently, NEA (153591) 2001 SN263 was chosen as the target of the ASTER MISSION – the First Brazilian Deep Space Mission, with launch planned for 2015. NEA (153591) 2001 SN263 was discovered in 2001. In 2008 February, radio astronomers from Arecibo-Puerto Rico concluded that (153591) 2001 SN263 is actually a triple system. The announcement of ASTER MISSION has motivated the development of the present work, whose goal is to characterize regions of stability and instability of the triple system (153591) 2001 SN263. Understanding and characterizing the stability of such a system is an important component in the design of the mission aiming to explore it. The method adopted consisted of dividing the region around the system into four distinct regions (three of them internal to the system and one external). We performed numerical integrations of systems composed of seven bodies, namely the Sun, Earth, Mars, Jupiter and the three components of the asteroid system (Alpha, the most massive body; Beta the second most massive body; and Gamma, the least massive body), and of thousands of particles randomly distributed within the demarcated regions, for the planar and inclined prograde cases. The results are displayed as diagrams of semi-major axis versus eccentricity that show the percentage of particles that survive for each set of initial conditions. The regions where 100 per cent of the particles survive are defined as stable regions. We found that the stable regions are in the neighbourhood of Alpha and Beta, and in the external region. Resonant motion of the particles with Beta and Gamma was identified in the internal regions, leading to instability. For particles with $I > 45^\circ$ in the internal region, where I is the inclination with respect to Alpha's equator, there is no stable region, except for particles placed very close to Alpha. The stability in the external region is not affected by the variation of inclination. We also present a discussion of the long-term stability in the internal region, for the planar and circular case, with comparisons with the short-term stability.

Key words: methods: N -body simulations – celestial mechanics – minor planets, asteroids.

1 INTRODUCTION

Asteroids are bodies that orbit the Sun but are too small to be considered as planets. As examples of primordial objects, they can help us to understand the process of formation of the Solar System. They can be classified according to their orbital characteristics, and according to their physical, chemical and mineralogical properties. An interesting group of asteroids is formed by the NEAs (near-

Earth asteroids), which, as the name suggests, designate asteroids that periodically approach the Earth's orbit.

NEAs belong to the group of NEOs (near-Earth objects), and up-to-date data from NASA show that they represent about 99 per cent of this population. NEAs are classified into four groups, according to their orbital characteristics, given by the perihelion (q), aphelion (Q) and semi-major axis (a), compared with the orbital characteristics of the Earth: aphelion $Q_T = 1.017$ au, perihelion $q_T = 0.983$ au and semi-major axis $a_T = 1.0$ au. The four groups are defined as follows. Apollo asteroids account for about 54.5 per cent of the population of NEOs. They have $q < Q_T$, $a > a_T$ and are on Earth-crossing orbits. Aten asteroids account for about 8.3 per cent of the population. They have $Q > Q_T$, $a < a_T$ and are also on

★E-mail: ran.araujo@gmail.com (RANA); ocwinter@pq.cnpq.br (OCW); prado@dem.inpe.br (AFBAP); sasha.su@hotmail.com (AS)

Earth-crossing orbits. Amor asteroids account for about 37.1 per cent of the population. They have $Q_T < q < 1.3$ au, $a > a_T$. They cross the orbit of Mars and approach the orbit of the Earth without crossing it. Finally the Atira asteroids, or IEO (interior to the Earth's orbit), account for about 0.1 per cent of the population and have $Q < q_T, a < a_T$. As the name suggests, they are NEOs with orbits internal to the orbit of Earth that do not cross it.

An interesting subgroup of asteroids is formed by binary and multiple systems. The first triple system of main-belt asteroids discovered was 87 Sylvia (Marchis et al. 2005). The dynamics of such a system were investigated by Winter et al. (2009).

Examination of doublet craters on Earth and Venus led Bottke & Melosh (1996) to suggest that about 15 per cent of the asteroids that cross the orbit of Earth are binaries. This suggestion was verified observationally by Margot et al. (2002) and Pravec et al. (2006). For Mars-crossing asteroids, the expected number is 5 per cent. Currently, 36 asteroids have been identified as multiple systems in the group of NEAs, 34 of them being binary systems, and only two being triple systems, namely (153591) 2001 SN263 (Amor; Nolan et al. 2008) and 1994 CC (Apollo; Brozovic et al. 2009), discovered in 2008 and 2009 respectively. Hereafter, we refer to the triple system (153591) 2001 SN263 by its provisional designation: 2001 SN263.

The NEOs are celestial bodies that represent a threat to life on Earth owing to the possibility of a catastrophic event caused by the impact of such a body with the surface of our planet. Thus, in addition to efforts to increase the number of known NEOs it is also important to know the composition of these bodies, to understand the processes that gave rise to them, and to examine how they evolve dynamically. Over the last few decades, there have been a number of studies that have explored these issues. Gladman, Michel & Froeschlé (2000) studied the lifetime of NEOs (about a few million years). Opik (1961) presented the first study aiming to explain the mechanism responsible for maintaining the population of NEOs, indicating a cometary origin for them. Later, the asteroidal origin of NEOs was considered, as discussed in Anders (1964), and it was concluded that some NEOs with high values of eccentricity and inclination were extinct nuclei of comets, while the remaining NEOs known at that time were main-belt asteroids that had reached typical NEO orbits by encounters with the planet Mars. In 2002, Morbidelli et al. (2002) showed how asteroids can escape from the asteroid belt through resonance mechanisms and supply the known population of NEOs. According to their study, only 6 per cent of the NEO population come from the Kuiper Belt (cometary origin).

In addition to the theoretical studies, as detailed above, space missions are an excellent way to increase our knowledge of asteroids. NEAs are good targets for such missions, as they periodically approach the orbit of the Earth. In this context, NEAs composed of two or three bodies (multiple asteroid systems) are especially interesting as they increase the range of possible observations and scientific results obtained by the mission. Because of these advantages a growing number of missions to NEAs have been completed or are being planned by the major aerospace agencies with these bodies as targets.

In 2003 May, the Japan Aerospace Agency launched the Hayabusa mission to NEA (25413) Itokawa, which reached its target in 2005 September. The same agency is planning a new mission called Hayabusa 2, targeting NEA 1999 JU3 and applying the same technology and concepts as in the first mission (Yoshikawa 2006). The European Space Agency (ESA) has performed some studies regarding missions to NEAs. The program Don Quijote (Galvez 2003) plans to launch two space vehicles. One of them will collide

with an NEA and the second will capture information about the internal structure of the asteroid. The program ISHTAR (D'arrigo 2003) plans to visit at least two NEAs and characterize all physical parameters of the asteroids, such as their mass distribution, density and surface properties. The SIMONE mission (Wells 2003) will be composed of five micro-satellites that will study individual NEAs of different classifications. The Marco Polo mission is also part of the program of ESA missions, and its main objective is to return to Earth carrying a sample of a NEA (Amata 2009). The HERA mission is a project being developed by the Arkansas Center for Planetary Science and the Jet Propulsion Laboratory. The goal is to send a probe to collect samples from three NEAs and then for it to return to Earth (Sears, Scheeres & Binzel 2004).

Recently, NEA 2001 SN263 was chosen as the target of the ASTER MISSION – the First Brazilian Deep Space Mission, with a planned launch date in 2015 (Sukhanov 2010). The target was chosen taking into account the advantages of sending a space probe to a multiple system of asteroids, which increases the range of possible scientific investigations (for example into the internal structure, formation process and dynamical evolution) with respect to the economy of fuel, flight time and telecommunication system required in comparison to a similar mission aimed at an asteroid of the main belt. The announcement of this project has motivated the present work, whose goal is to characterize the regions of stability and instability of the system. Such information is of great interest as it will serve as a parameter for the mission planning, and there are no previous works on this subject. The study was made through numerical integration of a system composed of seven massive bodies (Sun, Earth, Mars, Jupiter and the components of the triple system) and of thousands of particles randomly distributed around the three asteroids (internal region) and around the whole system (external region).

The structure of this paper is as follows. In Section 2 we present the triple system 2001 SN263. In Section 3 we discuss the initial conditions of the problem and the methodology adopted. In Section 4 we present a study of the stability in the internal region of the system for the planar case. In Section 5 we present a similar study considering the inclined prograde case. In Section 6 we discuss the resonant motion identified in the internal region. In Section 7 we present a study of the stability in the external region. In Section 8 we present an analysis of the long-term stability in the internal region, for the planar and circular cases. Finally, in Section 9 we make some final comments, with an overview of the results presented in the previous sections.

2 THE TRIPLE SYSTEM OF ASTEROID 2001 SN263

The asteroid 2001 SN263 was discovered in 2001 with the program LINEAR (Lincoln Near-Earth Asteroid Research) – a program developed jointly by the US Air Force, NASA and the Lincoln Laboratory. Light-curves obtained in the Observatory of Haute-Provence, in 2008 January, led to the conclusion that this asteroid was a binary system. In 2008 February, the system was observed for 16 days at the radio-astronomy station of Arecibo, in Puerto Rico. Those observations led to the discovery that 2001 SN263 is a triple system (Nolan et al. 2008). This is the first triple system known that approaches the orbit of the Earth and that crosses the orbit of Mars (Amor-type asteroid). In 2009 January, Becker et al. (2009) presented preliminary data on the physical aspects of the asteroids. Their study estimated that the primary (largest) body is approximately a spheroid with

Table 1. Physical and orbital data of the three components of the system 2001 SN263.

Body	Orbits	a^1	e^1	I^1 (*)	Period ¹	Radius	Mass ¹
Alpha	Sun	1.99 au	0.48	6.7°	2.80 yr	1.3 km^1	$M_\alpha = 917.47 \times 10^{10} \text{ kg}$
Beta	Alpha	16.63 km	0.015	$0^\circ 0'$	6.23 days	$0.39 \text{ km}^{(**)}$	$M_\beta = 24.04 \times 10^{10} \text{ kg}$
Gamma	Alpha	3.80 km	0.016	$\approx 14^\circ$	0.69 days	$0.29 \text{ km}^{(**)}$	$M_\gamma = 9.77 \times 10^{10} \text{ kg}$

¹Fang & Margot (2011).

(*) Inclination of Alpha related to the ecliptic plane. Inclinations of Beta and Gamma related to the equator of Alpha.

(**) Estimated values. From the mass and the radius of Alpha we calculated its density.

Assuming that Beta and Gamma have the same density as Alpha, and knowing their masses, we estimated their radius.



Figure 1. Representation of the triple system 2001 SN263. The blue circles represent the Hill’s radii of Beta and Gamma. The red dotted circles represent the collision-lines with Gamma and Beta, and, by definition, the limits of the internal regions.

principal axes of approximately 2.8 ± 0.1 , 2.7 ± 0.1 , 2.5 ± 0.2 km, and an estimated density of $1.3 \pm 0.6 \text{ g cm}^{-3}$.

In 2011, Fang & Margot (2011) presented a dynamical solution for both triple systems known in the group of NEAs, namely 2001 SN263 and 1994 CC. Using the data obtained through radar observations from Arecibo and Goldstone, and through numerical integrations of the N -body problem, they derived the masses of the components, the J_2 gravitational harmonic of the central bodies, and the orbital parameters of the satellites. The orbital and physical data for 2001 SN263 can be seen in Table 1.

Hereafter, we follow the nomenclature adopted by Fang & Margot (2011) for the triple system. We refer to the central body (the most massive body) as *Alpha*, to the second most massive body as *Beta* (outer) and to the least massive body as *Gamma* (inner). Fig. 1 is a representation of the system 2001 SN263.

3 REGIONS OF STABILITY

The triple system 2001 SN263 is an interesting system. It is composed of bodies with similar values of mass and radius, and they are close to each other. A particle placed in their neighbourhood experiences perturbations arising from all the bodies, and this will be decisive in determining the regions of stability and instability inside and outside the system.

The determination of a region of stability could indicate the location of a possible additional component of the system that has not yet been observed, or the location of small particles of debris. In contrast, an unstable region will be empty (no bodies or debris).

Such information is useful for the planning of a mission to the system, for example for the Brazilian mission cited previously.

We developed a method to determine the regions of stability in the neighbourhood of the components of the triple asteroid system 2001 SN263, in terms of orbital elements and within a given time-span, considering only the gravitational perturbation. In this first approach the effect of radiation pressure is not considered, although it is known that it may cause the removal of some small particles from the stable regions.

The initial conditions and the methodology adopted are described in the following subsections.

3.1 Initial conditions

We consider a system composed of seven massive bodies: the three components of the system 2001 SN263, the Sun and the planets Earth, Mars (owing to possible close encounters) and Jupiter (the system crosses the main asteroid belt). We introduce into the system thousands of particles, randomly distributed around the three asteroids as follow:

(i) Spatial distribution: the region around the three bodies was divided into four regions. We calculated Hill’s radius for the problems involving Alpha–Beta and Alpha–Gamma separately. This is an approximation, as the presence of the third body will change the values found; however, Hill’s radius is a good parameter to spatially delimit the regions in which each of the bodies is gravitationally dominant. The values found were $R_{\text{Hill}} \approx 3.4 \text{ km}$ for the primary bodies Alpha–Beta and $R_{\text{Hill}} \approx 0.6 \text{ km}$ for the primary bodies Alpha–Gamma. Fig. 1 is a representation of the asteroid system and of the Hill radius found for each body. The particles are spatially distributed in those regions. Region 1 is the region between Alpha and Gamma, with particles orbiting Alpha. Region 2 is the region between Gamma and Beta, with particles orbiting Alpha. Region 3 is the region where particles orbit Beta, limited by the Hill radius of this body. Region 4 is the region around Gamma, limited by the Hill radius of this body, and with particles orbiting Gamma.

(ii) All particles start with circular orbits ($e = 0.0$) until eccentricities are equal to 0.5.

(iii) Initially, only the planar case was considered (all particles with inclination $I = 0^\circ$ relative to the equator of the central body – Alpha). Subsequently, we performed the same analysis for particles with inclinations ranging from $I = 15^\circ$ to $I = 90^\circ$ (prograde cases).

(iv) Angularly, the particles were distributed with random values of the true anomaly ($0^\circ \leq f \leq 360^\circ$), the argument of the pericentre ($0^\circ \leq \omega \leq 360^\circ$) and the longitude of the ascending node ($0^\circ \leq \Omega \leq 360^\circ$).

(v) We considered the oblateness of the central body Alpha with a value of $J_2 = 0.013$ (Fang & Margot 2011). The obliquity of Alpha was also considered. It was determined through the pole solution given by Fang & Margot (2011).

3.2 Method

The method adopted involves the numerical integration of the equations of motion for a system composed of seven bodies (Sun, Mars, Earth, Jupiter and the triple system 2001 SN263) and of n particles (the number of particles will change for each region), for a time-span of 2 yr.

The orbits of the particles follow the conditions detailed in the previous subsection. The orbital elements of Beta and Gamma used as initial conditions in the integrations are given by Fang & Margot (2011). The data presented by them correspond to the epoch MJD 54509 in the equatorial frame of J2000. The orbital elements of the other bodies (Alpha, Earth, Mars and Jupiter) were obtained through JPL's Horizons system for the same epoch.

The time-span of 2 yr corresponds to ≈ 100 orbital periods of Beta and to ≈ 1000 orbital periods of Gamma, and is sufficient to guarantee the applicability of the results in the planning of the space mission to the system. The numerical integrations were performed with the Gauss–Radau numerical integrator (Everhart 1985). The time-step of the numerical integrations, for the internal and external regions, was 1 h (≈ 6 per cent of Gamma's orbital period).

Throughout the integration period we monitored the particles that collide with any of the bodies, and the particles ejected from the system. The collisions depend on the radius of the bodies, and the ejection is defined for each region. For region 1, the ejection distance is $d > 3.804$ km, which is an approximation and corresponds to the circular orbit of Gamma. Similarly, for region 2, the ejection distance is $d > 16.633$ km, which is also an approximation and corresponds to the circular orbit of Beta. The red dotted lines in Fig. 1 represent such ejection distances, and thus the limits of regions 1

and 2. For regions 3 and 4, the ejection distances are defined by the Hill radius of Beta and Gamma, respectively. So, $d > 3.4$ km for region 3 and $d > 0.6$ km for region 4.

The percentage of collisions and ejections define the regions of stability and instability of the system. The region of stability is defined as the region where 100 per cent of the particles survive for 2 yr. Below this value, we have instability.

4 PLANAR CASE

Here we present the results for each of the regions described in Section 3.1, considering only particles with $I = 0^\circ$ relative to the equator of Alpha.

Region 4 was not considered on the integrations. It is a very small region (≈ 0.6 km) and would become even smaller considering the gravitational influence of the third body (Beta). The particles would orbit very close to Gamma, increasing the collision probability.

Therefore, the internal regions considered were the regions 1, 2 and 3.

4.1 Region 1

In region 1, the particles orbit Alpha with orbital elements: $1.4 \leq a \leq 3.2$ km taken every 0.2 km, $0.0 \leq e \leq 0.50$ taken every 0.05, and 100 particles for each pair ($a \times e$), with random values for f , ω , Ω , as described in Section 3.1. Such a combination of values resulted in a total of 11, 000 particles placed in region 1, with $I = 0^\circ$.

Fig. 2(a) shows the results. It considers a grid of semi-major axis versus eccentricity, with each of the small 'boxes' holding the information of 100 particles that share the same initial values for a and e .

The diagram shows how many particles survive for each set of initial conditions. The coded colours indicate the percentage of survivors. Yellow indicates the initial conditions for which 90–100 per cent of particles survive for 2 yr. The yellow boxes marked with a

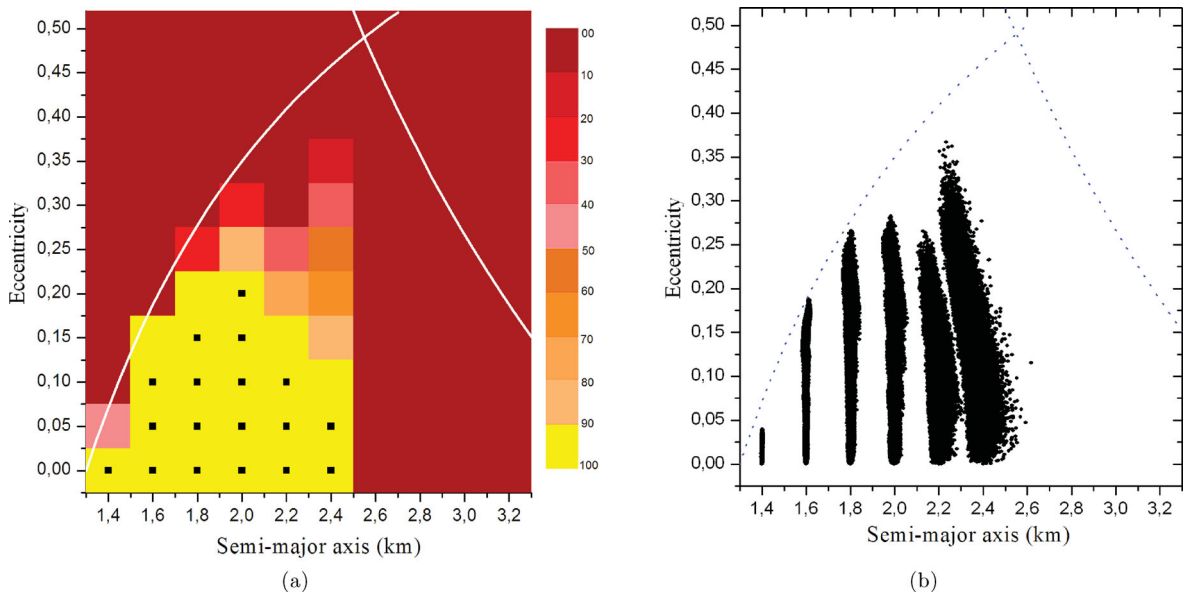


Figure 2. (a) Diagram of the stability of region 1, for a time-span of 2 yr. The scale goes from 0.0–10.0 per cent of particles surviving in that region (dark red) to 90–100 per cent survival (yellow). The yellow boxes marked with the small black squares indicate cases of 100 per cent survival. The white lines indicate the limits of the region. On the left is the collision-line with Alpha and on the right is the collision-line with Gamma, denoting the ejection distance d . (b) Scattering of particles in region 1. The diagram shows the evolution of a and e , throughout the 2 yr of integration, for every output step, for the particles belonging to the region with 90–100 per cent survival. The blue lines indicate the limits of the region.

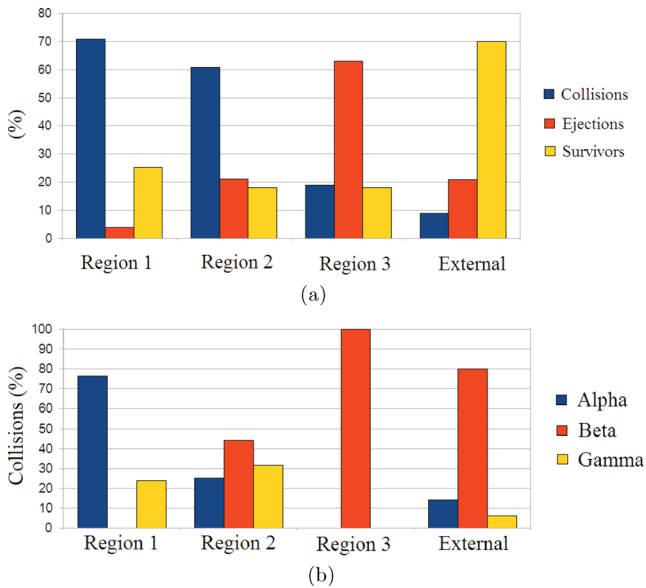


Figure 3. (a) Percentage of collisions, ejections and remaining particles for each region. (b) Percentage of collisions with each component of the triple system.

small black square indicate the specific cases where 100 per cent of the particles survive (stability). Dark red indicates the conditions for which fewer than 10 per cent of the particles survive for the same period.

As discussed in Section 3.2, if a particle in region 1 exceeds a distance of 3.804 km from Alpha, it is considered ejected. On the other hand, if such a distance is smaller than the radius of Alpha, we have collision. We can thus define the limits of the region, as represented in Fig. 2(a) by the white lines. On the right is the collision-line with Alpha. It gives the limit from which the pericentre (q) of the orbit of the particle is smaller than the radius of Alpha (R_{Alpha}). As $q = a(1 - e)$, from the collision conditions we have that $q \leq R_{\text{Alpha}}$, leading to the relation $a \leq R_{\text{Alpha}}/(1 - e)$, with $0.0 \leq e \leq 0.5$. On the left is the collision-line with Gamma, denoting the limit from which the apocentre (Q) of the orbit of the particle crosses the orbit of Gamma, and by definition, is beyond of the ejection distance d . As $Q = a(1 + e)$, the relation $a \geq d/(1 + e)$, with $0.0 \leq e \leq 0.5$, gives the limit of the collision-line with Gamma, for particles in region 1.

It can be seen from Fig. 2(a) that in region 1 the stable region is closer to Alpha for lower values of the eccentricity. As the value of the semi-major axis increases, the collisions with Gamma, or the ejections, become more frequent, giving rise to instability. A similar behaviour occurs when the value of eccentricity increases and the orbits of the particles approach the collision-line with Alpha.

Fig. 2(b) shows the scattering of the particles in region 1. It shows the evolution of a and e throughout the 2 yr of integration, for every output step, for the surviving particles belonging to the region where there was 90–100 per cent survival (yellow). We see that, in fact, the particles are confined within the limits of the region (blue lines). Apart from that, there is almost no variation of the semi-major axis. The external particles are the most perturbed, as expected.

Fig. 3(a) shows the percentage of collisions, ejections and survivors for the internal and external regions. Fig. 3(b) shows the percentage of collisions of the particles with each of the bodies of the triple system in such regions. From these figures it can be

seen that the number of ejections of particles in region 1 is very low. Owing to their proximity to both massive asteroids, Alpha and Gamma, the collisions are more frequent, mainly with Alpha.

4.2 Region 2

In region 2, the particles are orbiting the asteroid Alpha with semi-major axis $4.5 \leq a \leq 13.5$ km, taken every 0.2 km, and $0.0 \leq e \leq 0.50$, taken every 0.05. For each pair ($a \times e$), there are 100 particles with random values for f , ω , Ω and initial inclination $I = 0^\circ$. Such a combination of values resulted in a total of 50 600 particles placed in region 2.

Similar to in Fig. 2, Fig. 4 shows the region of stability found for region 2. As before, a grid of semi-major axis versus eccentricity was adopted. The details of the grid are given in Section 4.1.

As discussed in Section 3.2, if a particle in region 2 exceeds a distance of $d = 16.633$ km from Alpha it is considered ejected. For distances near 3.804 km, however, the particles cross the orbit of Gamma, increasing the collision probability, even with Alpha. We represent such limits by the white lines in Fig. 4(a). On the left is the collision-line with Gamma for particles in region 2. It gives the limit from which the pericentre (q) of the orbit of the particle is smaller than $d = 3.804$ km. As $q = a(1 - e)$, we have the relation $a \leq d/(1 - e)$, with $0.0 \leq e \leq 0.5$. On the right is the collision-line with Beta, denoting the limit from which the apocentre (Q) of the orbit of the particle crosses the orbit of Beta, and, by definition, is beyond the ejection distance $d = 16.633$ km. As $Q = a(1 + e)$, the relation $a \geq d/(1 + e)$, with $0.0 \leq e \leq 0.5$, gives the limit of the collision-line with Beta for particles in region 2.

It can be seen from Fig. 4(a) that almost no particle survives for 2 yr in the region between the asteroids Gamma and Beta. Better results are found approximately in the middle of the region for lower values of eccentricities, and the condition of 100 per cent of survival was reached only for three specific values of semi-major axis ($a = 9.1, 9.5, 9.7$ km) for $e = 0.0$. The observed instability can be explained by the fact that region 2 is a region surrounded by massive bodies, and also by the presence of resonant motion of the particles with Gamma or Beta, characterized by the gap near the centre of the region. This is discussed in Section 6.

Fig. 4(b) shows the scattering of the particles in region 2. It shows the evolution of a and e of the surviving particles, belonging to the region where there was 90–100 per cent survival (yellow), throughout the 2 yr of integration for every output step. Again we confirm that the particles are confined within the limits of the region (blue lines).

In region 2 the collisions still prevail over the ejections, as can be seen in Fig. 3(a), and the collisions with Beta are more frequent (Fig. 3b).

4.3 Region 3

In region 3, the particles are orbiting Beta with semi-major axis $0.8 \leq a \leq 3.4$ km, taken every 0.2 km, and $0.0 \leq e \leq 0.50$, taken every 0.05. For each pair ($a \times e$), there are 100 particles with random values for f , ω , Ω , with initial inclination $I = 0^\circ$. Such a combination of values resulted in a total of 15 400 particles placed in region 3.

Fig. 5(a) shows the region of stability found for region 3. As before, a grid of semi-major axis versus eccentricity was adopted. The details of the grid are given in Section 4.1. Similar to what happens in region 1, the region where more particles survive in

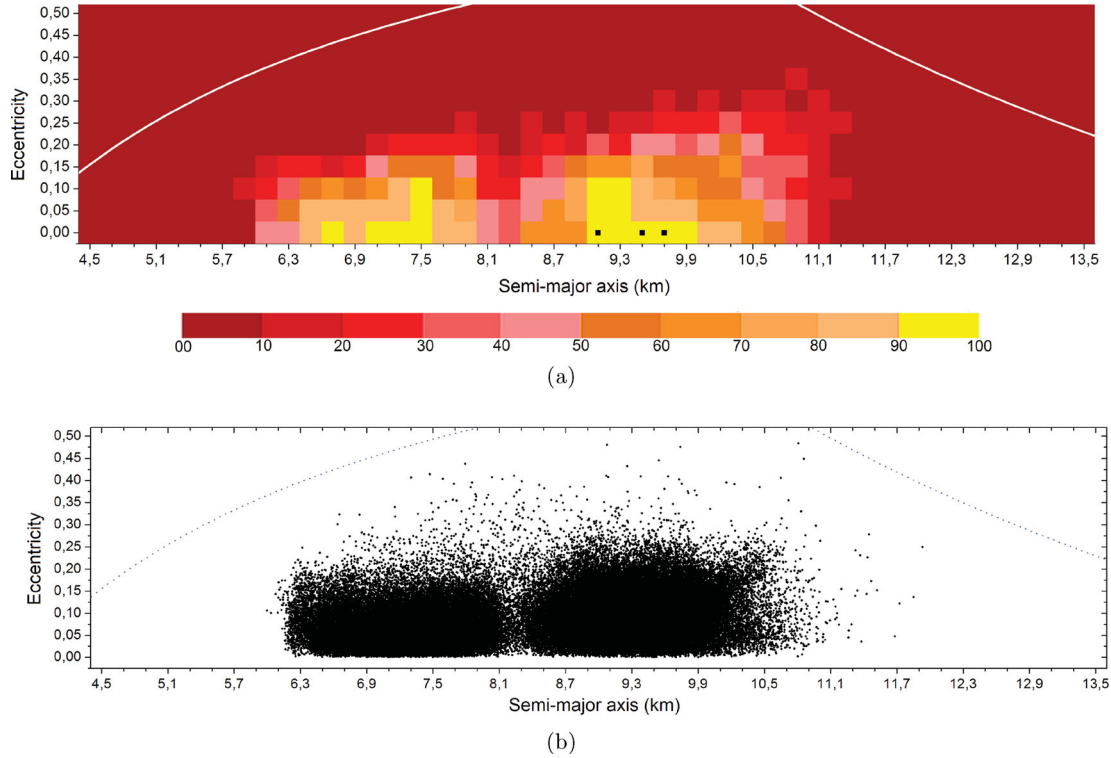


Figure 4. (a) Stability of region 2, for a time-span of 2 yr. The scale goes from 0.0–10.0 per cent of particles surviving in that region (dark red) to 90–100 per cent survival (yellow). The yellow boxes marked with the small black squares indicate cases of 100 per cent survival. The white and blue lines indicate the limits of the region. On the left is the collision-line with Gamma, for particles in region 2. On the right is the collision-line with Beta, denoting the ejection distance. (b) Scattering of the particles in region 2. The diagram shows the evolution of a and e , throughout the 2 yr of integration, for every output step, for the particles belonging to the region with 90–100 per cent survival. The blue lines indicate the limits of the region.

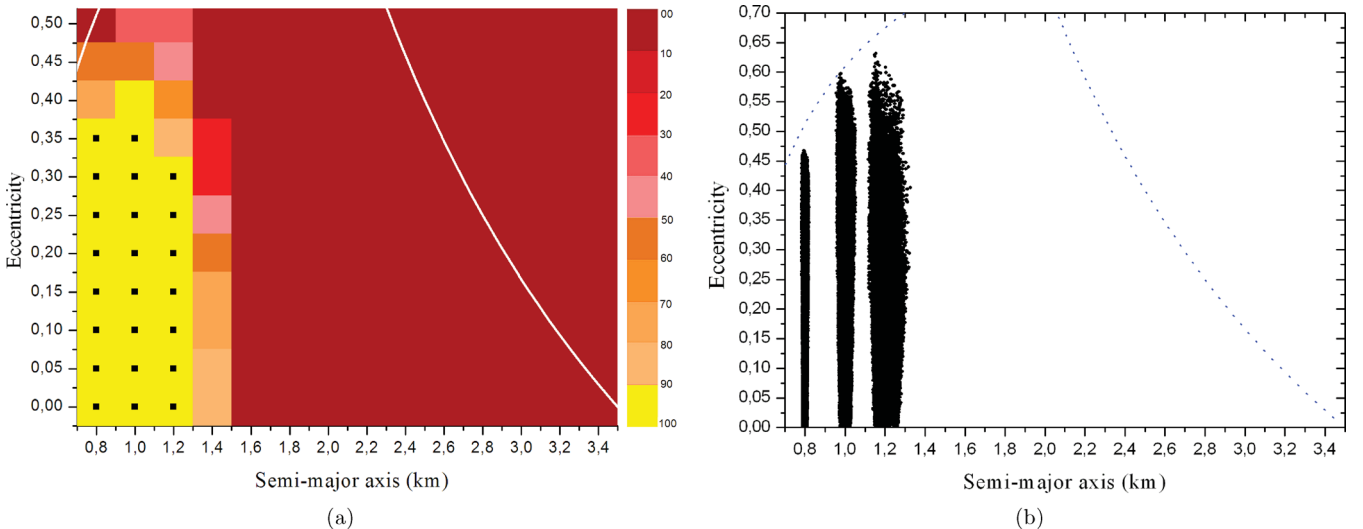


Figure 5. (a) Stability of region 3, for a time-span of 2 yr. The scale goes from 0.0–10.0 per cent of particles surviving in that region (dark red) to 90–100 per cent survival (yellow). The yellow boxes marked with the small black squares indicate cases of 100 per cent survival. The white lines indicate the limits of the region. On the left is the collision-line with Beta, and on the right is the ejection-line. (b) Scattering of particles in region 3. The diagram shows the evolution of a and e , throughout the 2 yr of integration, for every output step, for the particles belonging to the region with 90–100 per cent survival. The blue lines indicate the limits of the region.

region 3 is that closer to the asteroid that they orbit, in this case Beta.

As discussed in Section 3.2, if a particle in region 3 exceeds a distance of 3.4 km from Beta it is considered ejected. If such a distance is smaller than the radius of Beta, however, we have

collision. So, the white lines in Fig. 4(a) define the limits of region 3. On the right is the collision-line with Beta. It gives the limit at which the pericentre (q) of the orbit of the particle is smaller than the radius of Beta (R_{Beta}). As $q = a(1 - e)$, from the collision conditions we have that $q \leq R_{\text{Beta}}$, leading to the relation $a \leq R_{\text{Beta}}/(1 - e)$,

with $0.0 \leq e \leq 0.5$. On the left is the ejection-line, denoting the limit at which the apocentre (Q) of the orbit of the particle is greater than the ejection distance $d = 3.4$ km. As $Q = a(1 + e)$, the relation $a \geq d/(1 + e)$, with $0.0 \leq e \leq 0.5$, gives the limit of ejection for particles in region 3.

As presented for regions 1 and 2, Fig. 5(b) shows the scattering of the particles in region 3 throughout the 2 yr of integration, for every output step. We see that there is almost no variation of the semi-major axis. The external particles are the most perturbed, and almost no particles survive in the region beyond half a Hill's radius (≈ 1.7 km).

According to Fig. 3(a), the number of ejections increases in region 3, which makes sense, as Beta is the outermost body of the system. From the definition of region 3, collisions can happen only with Beta (Fig. 3b).

5 INCLINED PROGRADE CASE

Now that we have discussed the planar case, we are going to consider inclined particles orbiting the same internal regions. The purpose is to analyse what changes occur to the stable regions found in the planar case (Section 4) when the particles have an inclination relative to the equator of the central body. For all three internal regions, the initial conditions and the number of particles are exactly the same, except that the inclination of the particles varies from 15° to 90° in fixed intervals of 15° (six cases for each region). The results are presented in the following subsections.

5.1 Region 1

As in the planar case, the particles are orbiting Alpha with $1.4 \leq a \leq 3.2$ km, taken every 0.2 km, $0.0 \leq e \leq 0.50$, taken every 0.05, random values for f , ω , Ω and now with a variation in inclination: $15^\circ \leq I \leq 90^\circ$ taken every 15° .

The regions of stability found for the inclined prograde case in region 1 are presented in Fig. 6. Again a diagram of semi-major axis versus eccentricity was adopted. The limits of the region marked by the white lines are the same as discussed in Section 4.1.

The region of stability found in region 1 for the planar case remains for the cases with inclination until the critical value $I = 60^\circ$, when the stable region decreases significantly. This phenomenon is attributed to the Kozai mechanism (Kozai 1962). In region 1, the particles with $I = 60^\circ$ have an inclination relative to the orbital plane of Gamma of $\sim 46^\circ$. Therefore, such particles exceed the *critical angle of Kozai* given by $I_{\text{crit}} \approx 39:2$. A known effect of the Kozai mechanism is the generation of oscillations of the eccentricity and of the mutual inclinations. These oscillations increase the probability of close encounters and collisions, and lead to the observed instability for larger values of inclination in region 1. An exception occurs for $I = 90^\circ$, for which a slight increase of the stable region is observable (Delsate et al. 2010).

Fang & Margot (2012) presented a discussion of the role of the Kozai mechanism in binary NEAs. They considered a system composed of the Sun and a binary system. In their model the secondary body orbits on the equatorial plane of the primary. The pole orientation of the primary is such that the relative inclination between the mutual orbit of components of the binary and the heliocentric orbit of the binary system is in the interval $39:2 < I < 140:8$. The Sun is the perturber, and the authors analysed the perturbations experienced by the secondary body owing to the Kozai mechanism

and how the J_2 of the primary affects this problem. They found that for a close binary the Kozai cycles cannot occur. They showed that the precession of the pericentre of the secondary body owing to the oblateness of the primary is enough to suppress the effects arising from the Kozai mechanism, even for very small J_2 values.

Considering their results, it would be expected for our case that the particles in region 1, placed close to Alpha (less than 3 radii of the primary), would experience the same kind of effect, namely that the pericentre precession of the particles resulting from the oblateness of Alpha would suppress the effects arising from the Kozai mechanism. Nevertheless, we found that the particles in such a region present the expected Kozai behaviour, such as libration of the argument of pericentre and an increase of the eccentricity while the inclination decreases (Delsate et al. 2010). Only the particles really close to Alpha do not present such Kozai behaviour; that is, their argument of pericentre circulates and the eccentricity and inclination suffer a small variation, leading to stability (see Fig. 6d for $a = 1.4$ and 1.6 km, for instance).

Thus, as discussed by Fang & Margot (2012), we also found that the primary oblateness is capable of suppressing the action of the Kozai mechanism, and that this depends on the distance of the perturbed body from the primary. However, the distances found for which each regime dominates are different from the distances found in the cited work. This is mainly because in our system the particles are not placed in the equatorial orbital plane of the primary, in contrast to the case in the cited model.

Analysing the equation that gives the precession rate of the argument of pericentre due to J_2 (Roy 1988), we see that the maximum value occurs when the inclination of the perturbed body to the equatorial plane is zero. When the perturbed body has a relative inclination different from zero, the precession rate of the argument of the pericentre decreases, and thus the ability of the oblateness of the primary body to suppress the Kozai mechanism also decreases. As a consequence, the particles have to be closer to the primary to be stable, and particles slightly farther away will be unstable. That is what we observe for the particles in the internal region of the triple system 2001 SN263. They are not placed in the equatorial plane, and so they are not affected by J_2 as much as they would be if they were in a non-inclined orbit.

Fig. 6 also reveals the occurrence of a gap in the stable region as the inclination increases, located at $a = 1.8$ km. Such behaviour has the characteristics of a resonance and is discussed in Section 6.

5.2 Region 2

As in the planar case, the particles are orbiting Alpha with semi-major axis $4.5 \leq a \leq 13.5$ km, taken every 0.2 km, and $0.0 \leq e \leq 0.50$, taken every 0.05, but now with a variation in inclination: $15^\circ \leq I \leq 90^\circ$ taken every 15° . The other orbital elements were chosen in the same way as before.

The regions of stability found for the inclined prograde case in region 2 are presented in Fig. 7. Comparisons between these diagrams and the diagram for the planar case (Fig. 4) show a similar behaviour, with distinct stable regions in the middle of the region and a gap approximately at the centre indicating the presence of a resonance, discussed in Section 6.

From the same diagrams we see that, similar to what is observed for region 1, there is no stable region for $I \geq 60^\circ$, an indication of the Kozai mechanism, which increases the eccentricities of the particles until they reach the collision or the ejection limit.

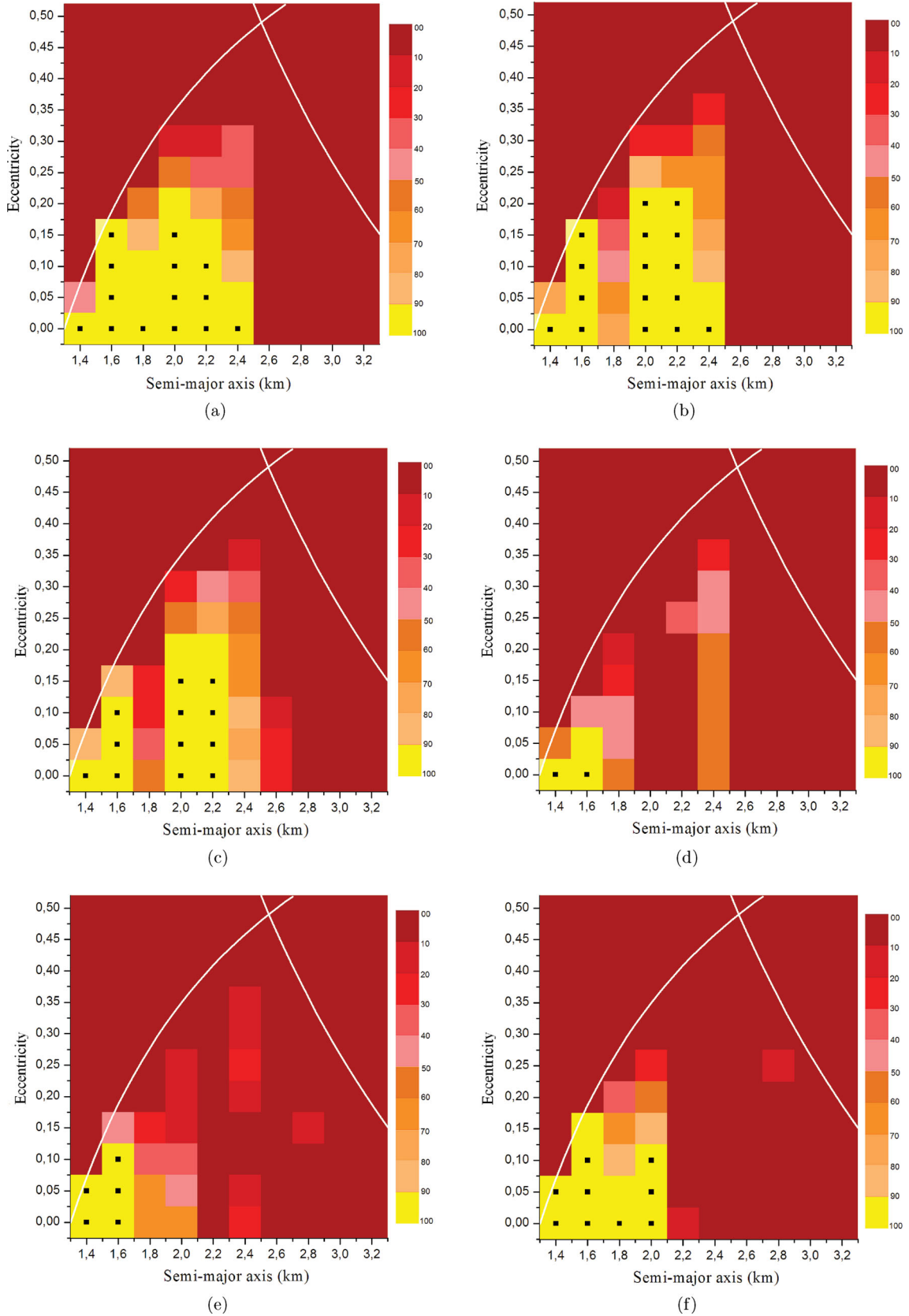


Figure 6. Stability of region 1, for a time-span of 2 yr. (a) $I = 15^\circ$, (b) $I = 30^\circ$, (c) $I = 45^\circ$, (d) $I = 60^\circ$, (e) $I = 75^\circ$, (f) $I = 90^\circ$. The white lines indicate the limits of the region. The yellow boxes marked with the small black squares indicate cases of 100 per cent survival.

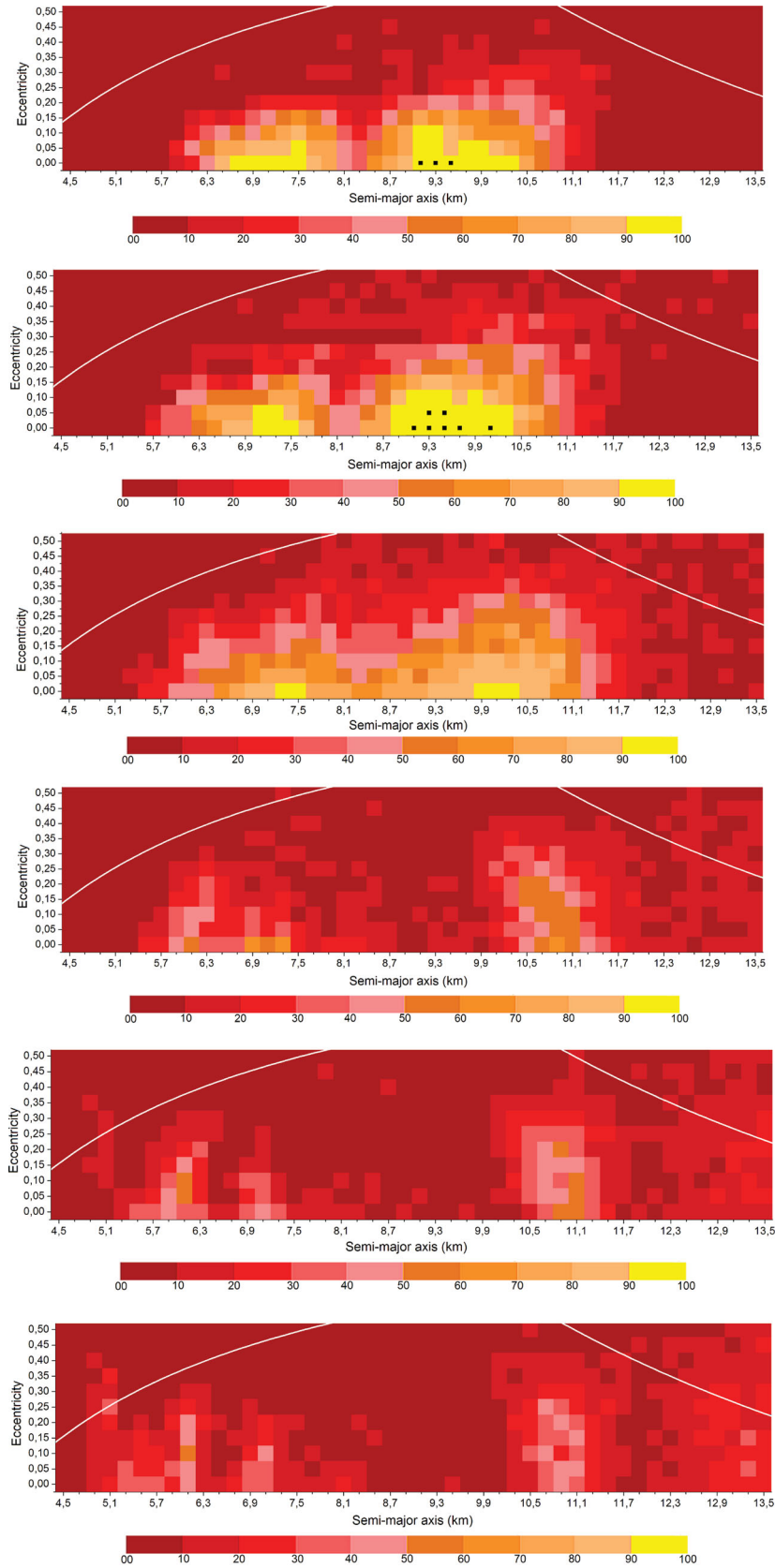


Figure 7. Stability of region 2, for a time-span of 2 yr for $I = 15^\circ, I = 30^\circ, I = 45^\circ, I = 60^\circ, I = 75^\circ$ and $I = 90^\circ$. The white lines indicate the limits of the region. The yellow boxes marked with the small black squares indicate the cases of 100 per cent of survival.

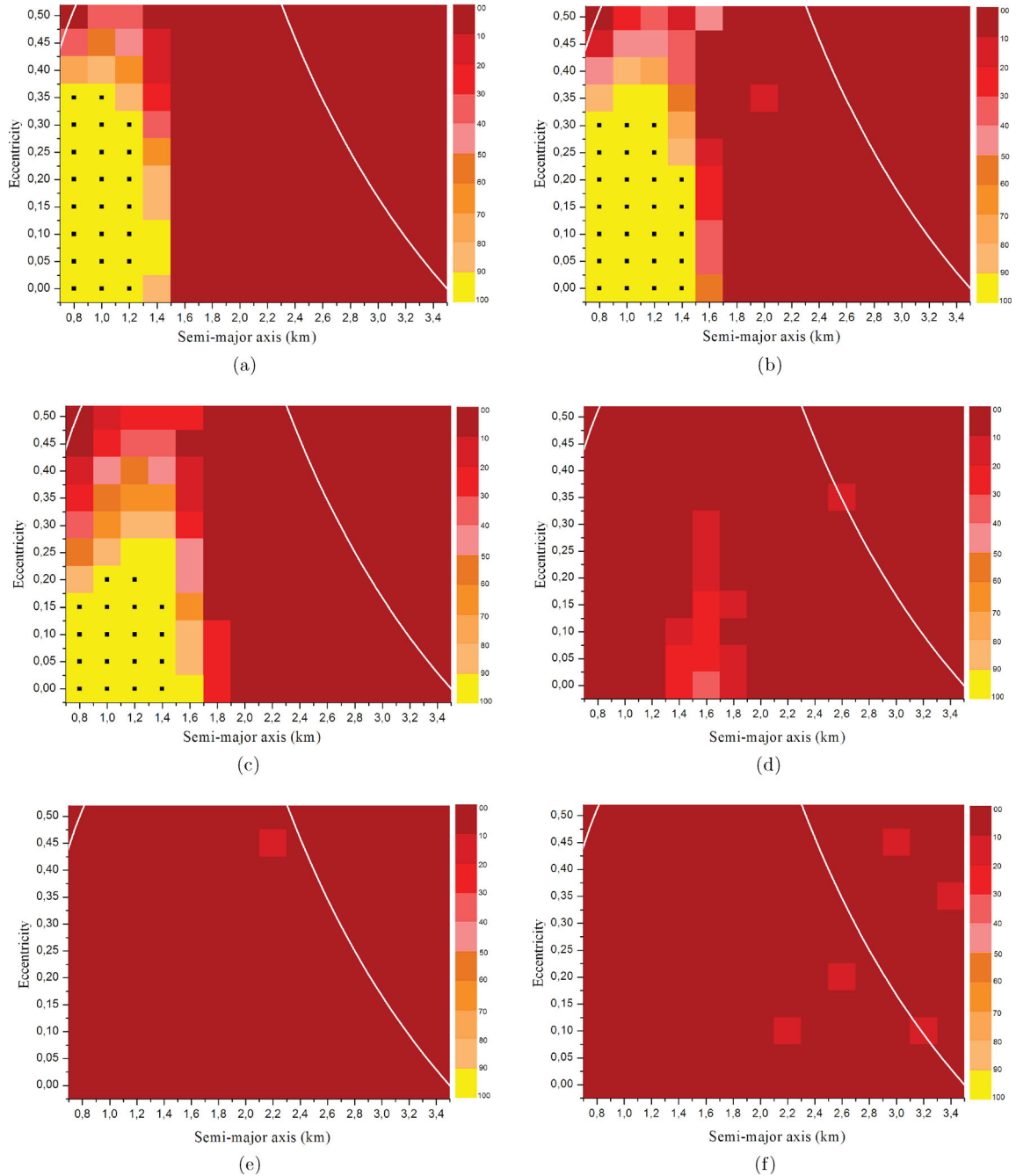


Figure 8. Stability of region 3, for a time-span of 2 yr. (a) $I = 15^\circ$, (b) $I = 30^\circ$, (c) $I = 45^\circ$, (d) $I = 60^\circ$, (e) $I = 75^\circ$, (f) $I = 90^\circ$. The white lines indicate the limits of the region. The yellow boxes marked with the small black squares indicate the cases of 100 per cent survival.

5.3 Region 3

As in the planar case, in region 3 the particles are orbiting Beta with semi-major axis $0.8 \leq a \leq 3.4$ km, taken every 0.2 km, with a variation in inclination of $15^\circ \leq I \leq 90^\circ$, taken every 15° . The other orbital elements were chosen in the same way as before.

The diagrams of semi-major axis versus eccentricity in Fig. 8 show that, for particles in region 3 with inclination ranging from $I = 0^\circ$ to $I = 45^\circ$, the stable region is approximately the same as before, with particles very close to Beta, even for particles with high eccentricities.

Similar to what happens to the particles in region 2, there is no stable region for inclinations higher than 60° , an effect of the Kozai mechanism.

6 INTERNAL REGIONS: RESONANT MOTION

Analysis of the stability diagrams in Figs 6 and 7 reveals the development of gaps in the internal regions 1 and 2 ($a \approx 1.8$ km for region 1 and $a \approx 8.0$ km for region 2). Such behaviour has the characteristics of possible resonant motions between the particles and Gamma or Beta in thin regions. We have investigated this, and the discussions are presented below.

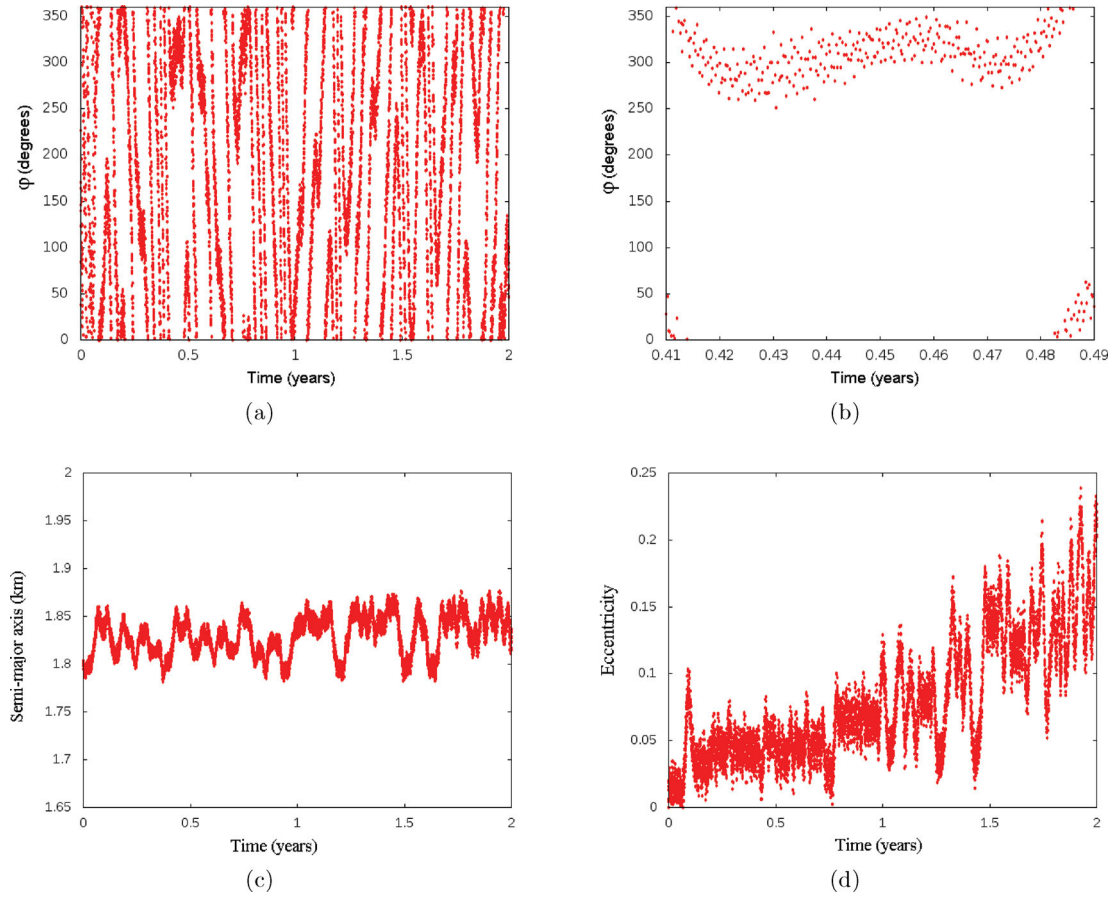


Figure 9. Particle in region 1 with $a = 1.8$ km, $e = 0.0$, $I = 15^\circ$. (a) Evolution of the resonant angle $\varphi = 3\lambda - \lambda' - \varpi' - \Omega'$ for $t = 2$ yr. (b) Zoom of (a) showing one of the libration regions, with time going from 0.41 to 0.49 yr (~ 42 orbital periods of Gamma). (c) Evolution of semi-major axis. (d) Evolution of eccentricity.

6.1 Resonance in region 1

In order to characterize the resonant motion of the particles in region 1 with Gamma or Beta, we first performed a search for the commensurabilities of mean motion. The mean motions of the particles and of the satellites were determined through equation (1), considering the oblateness of the central body and the semi-major axis of the involved bodies (Murray & Dermott 1999):

$$n = \frac{Gm_p}{a^3} \left[1 + \frac{3}{2} J_2 \left(\frac{R_p}{a} \right)^2 \right] \quad (1)$$

where G is the constant of gravitation, and m_p and R_p are the mass and the radius of the primary, respectively.

Our analysis shows that the particles located at $a = 1.8$ km are in a 3:1 commensurability of mean motion with Gamma. Knowing this relationship, it is necessary to determine the coefficients j_i ($\sum_{j=1}^6 j_i = 0$), for which the resonant angle

$$\varphi = j_1\lambda' + j_2\lambda + j_3\varpi' + j_4\varpi + j_5\Omega' + j_6\Omega \quad (2)$$

is librating, showing that the bodies are in resonance. In equation (2), λ is the mean longitude, ϖ is the longitude of the pericentre and Ω is the longitude of the ascending node of the satellite, while λ' , ϖ' and Ω' are related to the particle.

We found, considering a particle in region 1 with $a = 1.8$ km, $e = 0.0$ and $I = 15^\circ$, that the resonant angle $\varphi = 3\lambda - \lambda' - \varpi' - \Omega'$ presents an intermittent behaviour (circulating and librating),

as shown in Figs 9(a) and (b). Therefore, particles in such a neighbourhood experience the effects of a 3:1 resonance with Gamma. As a consequence, the particles in this region are perturbed in such a way that the semi-major axis remains almost constant while the eccentricity increases (Figs 9c and d), and then the particles cross the collision-line of the region, giving rise to the observable instability.

6.2 Resonances in region 2

An investigation similar to the analysis performed for region 1 shows that particles in region 2, with $a \approx 8.0$ km, are in a 3:1 commensurability of mean motion with Beta. Particles with $a \approx 7.9$ km, in the same region, are in a 1:3 commensurability of mean motion with Gamma.

For the resonance with Beta, we found that the resonant angle $\varphi = 3\lambda - \lambda' - \varpi' - \Omega'$ shows an intermittent behaviour (circulating and librating), as shown in Figs 10(a) and (b). Therefore, particles in such a neighbourhood experience the effects of a 3:1 resonance with Beta. As a consequence, the particles in this region are perturbed in such a way that the semi-major axis remains almost constant while the eccentricity increases (Figs 10c and d), and then the particles cross the collision-line of the region, giving rise to the observable instability. A similar behaviour was found for the 1:3 resonance with Gamma for the resonant angle $\varphi = 3\lambda' - \lambda - \varpi - \Omega$, as can be seen in Fig. 11.

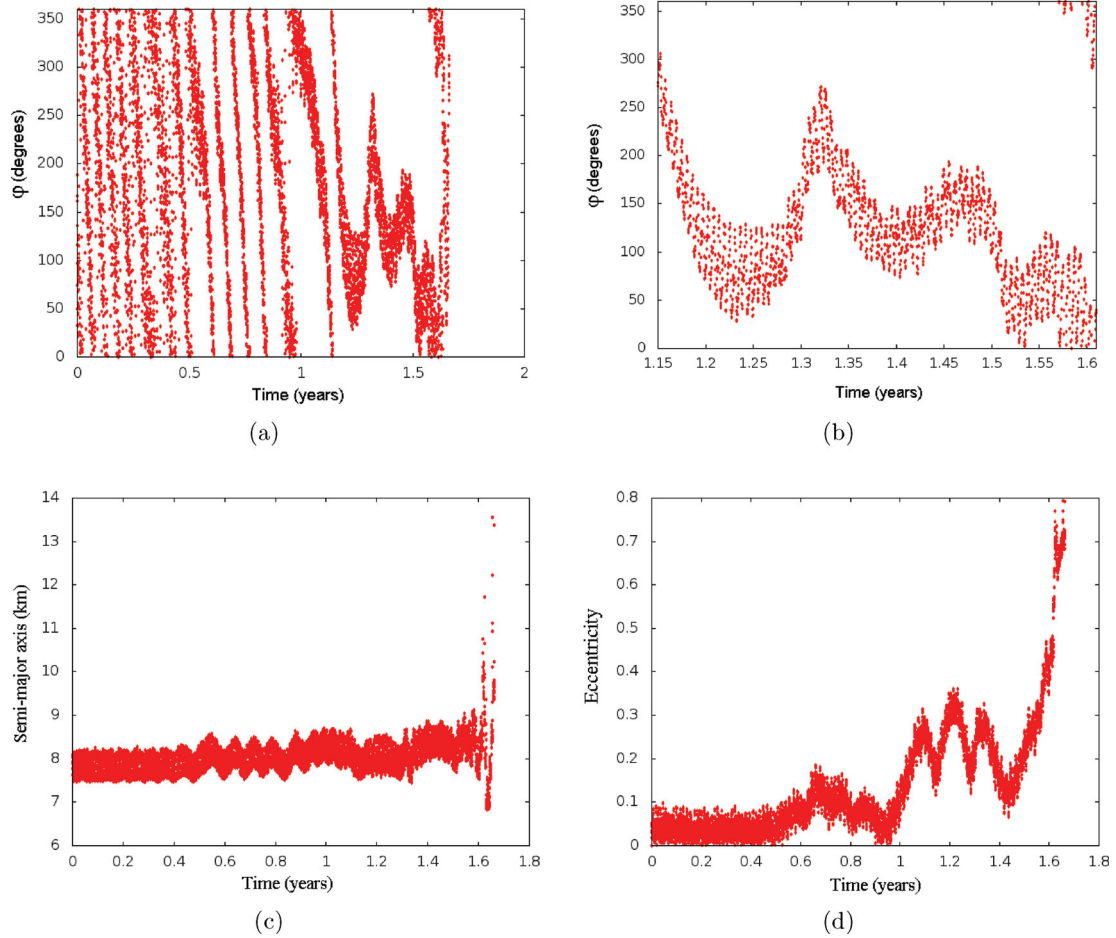


Figure 10. Particle in region 2 with $a = 7.9$ km, $e = 0.0$, $I = 0^\circ$ that collides with Gamma at $t \approx 1.6$ yr. (a) Evolution of the resonant angle $\varphi = 3\lambda - \lambda' - \varpi' - \Omega'$ for $t \approx 1.6$ yr. (b) Zoom of (a) showing the large libration region, with time going from 1.35 to 1.5 yr (~ 9 orbital periods of Beta). (c) Evolution of semi-major axis. (d) Evolution of eccentricity.

7 THE EXTERNAL REGION

In the previous sections we characterized the stability of the internal regions of the triple system 2001 SN263 for the planar and inclined prograde cases. Now we extend our analysis to the external region.

The methodology adopted is the same as before; that is, we performed numerical integrations for thousands of particles orbiting Alpha, but now with orbits external to the system. To obey such conditions the particles must be more distant from Alpha than Beta (lower limit). The upper limit is defined taking into account the approximated Hill radius of the whole system. Considering a body whose mass is equal to the sum of the mass of Alpha, Beta and Gamma, and the orbit of the system relating to the Sun, we have calculated that Hill's radius of such a hypothetical body is $R_{\text{Hill}} \approx 180.0$ km at perihelion of the orbit and $R_{\text{Hill}} \approx 500.0$ km at aphelion. According to Domingos, Winter & Yokoyama (2006), the limit of stability is about half a Hill's radius for prograde cases. Thus, the value for the upper limit of the external region was chosen to be $d = 90.0$ km ($\approx 0.5R_{\text{Hill}}$ at perihelion, when the system is more perturbed). Beyond the distance d , the particles are considered ejected. Collisions with all of the bodies are also considered.

Based on such limits we have the initial conditions for the particles in the external region, namely $20.0 \leq a \leq 90.0$ km, taken every 1.0 km, $0.0 \leq e \leq 0.50$, taken every 0.05, and 100 particles for each pair ($a \times e$) with random values for f , ω , Ω . The combination of

these initial conditions resulted in 78 100 particles placed in such a region.

We performed numerical integration using the Gauss–Radau integrator for a time-span of 2 yr of the problem consisting of these particles and seven massive bodies: the Sun, the planets Earth, Mars and Jupiter, and the triple system of the asteroid, considering again the planar case ($I = 0^\circ$) and the inclined prograde cases $15^\circ \leq I \leq 90^\circ$. The results are presented in the following subsections.

7.1 Planar case

The regions of stability found for the external region, for the planar case, are presented in the first diagram of Fig. 12. As before, a grid of semi-major axis versus eccentricity was considered, and each small ‘box’ holds the information of 100 particles that share the same initial values for a and e . The coded colour indicates the percentage of survivors, as previously defined.

The limits of the region are represented in the diagram by the white lines. On the left is the collision-line with Beta, which can also be understood as the limit between the internal and external regions, according to their definitions. Considering that the limit of the internal region is given by $d = 16.633$ km, and that $q = a(1 - e)$ gives the distance of the particles to Alpha at the pericentre, then, the relation $a = d/(1 - e)$ numerically gives the limit from which the particles cross the orbit Beta. On the right is the

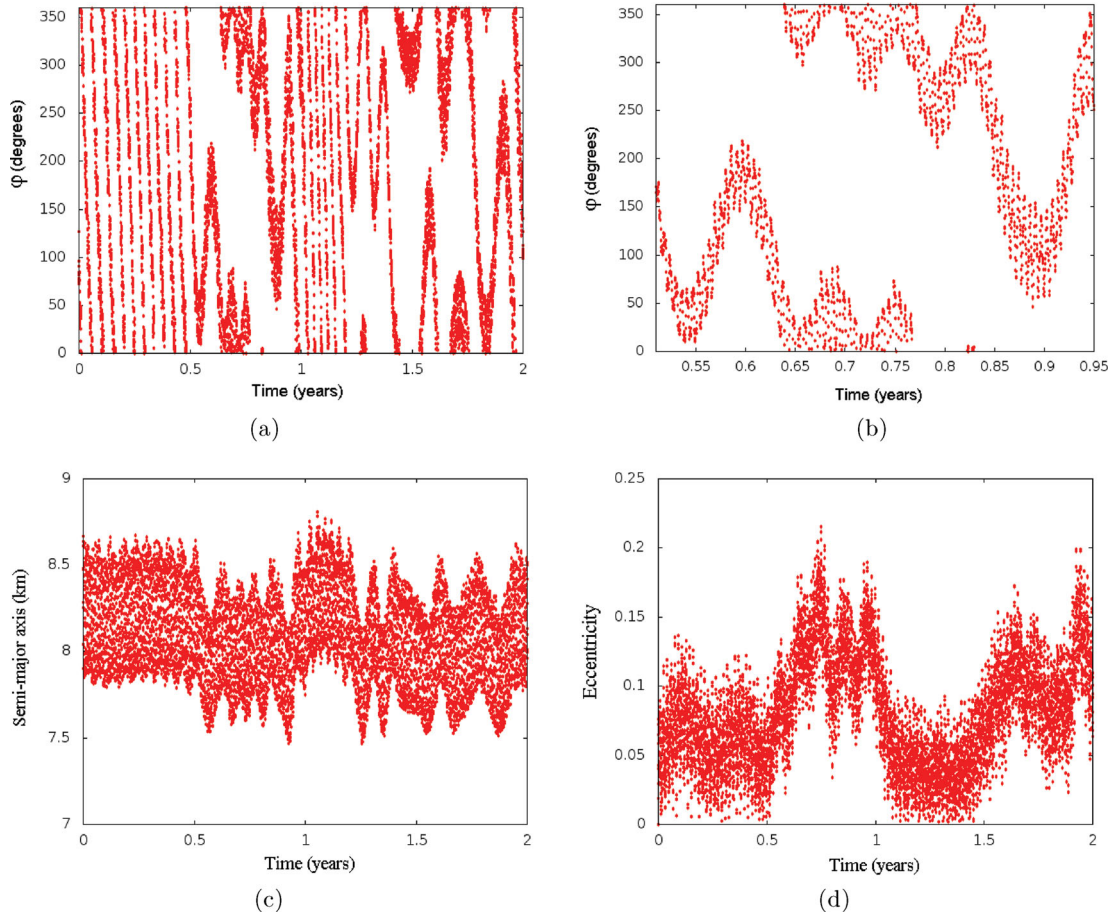


Figure 11. Particle in region 2 with $a = 7.9$ km, $e = 0.0$, $I = 0^\circ$. (a) Evolution of the resonant angle $\varphi = 3\lambda' - \lambda - \varpi - \Omega$ for $t = 2$ yr. (b) Zoom of (a) showing one of the libration regions, with time going from 0.85 to 0.92 yr (~ 37 orbital periods of Gamma). (c) Evolution of semi-major axis. (d) Evolution of eccentricity.

ejection-line, denoting the limit at which the apocentre (Q) of the orbit of the particle is greater than the ejection distance $d = 90.0$ km. As $Q = a(1 + e)$, the relation $a = d/(1 + e)$, with $0.0 \leq e \leq 0.5$, gives the limit of ejection for the external region.

From such a diagram of stability we see that the unstable regions are found beyond the limit of the ejection-line, and in the neighbourhood of Beta, caused mostly by the collisions of the particles with this body, as can be seen in Fig. 3. According to the same figure, about 30 per cent of the particles collide or are ejected.

Approximately 27 per cent of the particles are in the region where 100 per cent of the particles survive for 2 yr (yellow region marked with the small black squares); hence, the stable region is predominant in the external region.

7.2 Inclined prograde case

The initial conditions, the number of particles and the limits of the region are exactly the same as for the planar case, except for the inclination of the particles, which is taken from 15° to 90° at a fixed interval of 15° . The stable regions found for these conditions are presented in Fig. 12.

Comparing these diagrams with each other, and with the diagram for the planar case, we conclude that the stable regions are almost the same, and so the variation of inclination does not affect the stability of the external region of the triple system.

8 LONG-TERM STABILITY – PLANAR AND CIRCULAR CASE

Here we present a study of the long-term stability for the planar and circular case, in the internal region. We restricted our analysis to this special case because it is more interesting from the point of view of a spacecraft mission, and also because of the substantial computational processing time required to perform long-term stability integrations for the eccentric and inclined cases as well as for the particles placed in the external region.

We performed numerical integrations considering particles with $e = 0.0$, $I = 0^\circ$ from regions 1, 2 and 3 belonging to the set of initial conditions that resulted in 100 per cent survival (yellow region marked with the small black squares), for a time-span of 2000 yr.

The period of 2000 yr corresponds to approximately 700 orbital periods of Alpha, 106.000 orbital periods of Beta, and a million orbital periods of Gamma. Throughout this period there were no close encounters (within 1 Hill radius) between the system and the planets Earth and Mars. Nevertheless, the period of 2000 yr is sufficient to capture the effects of the secular perturbations experienced by the system.

The results found for each of the internal regions are presented in Fig. 13. From the figure we make a comparison between the percentages of survivors after 2 yr and after 2000 yr, for each initial

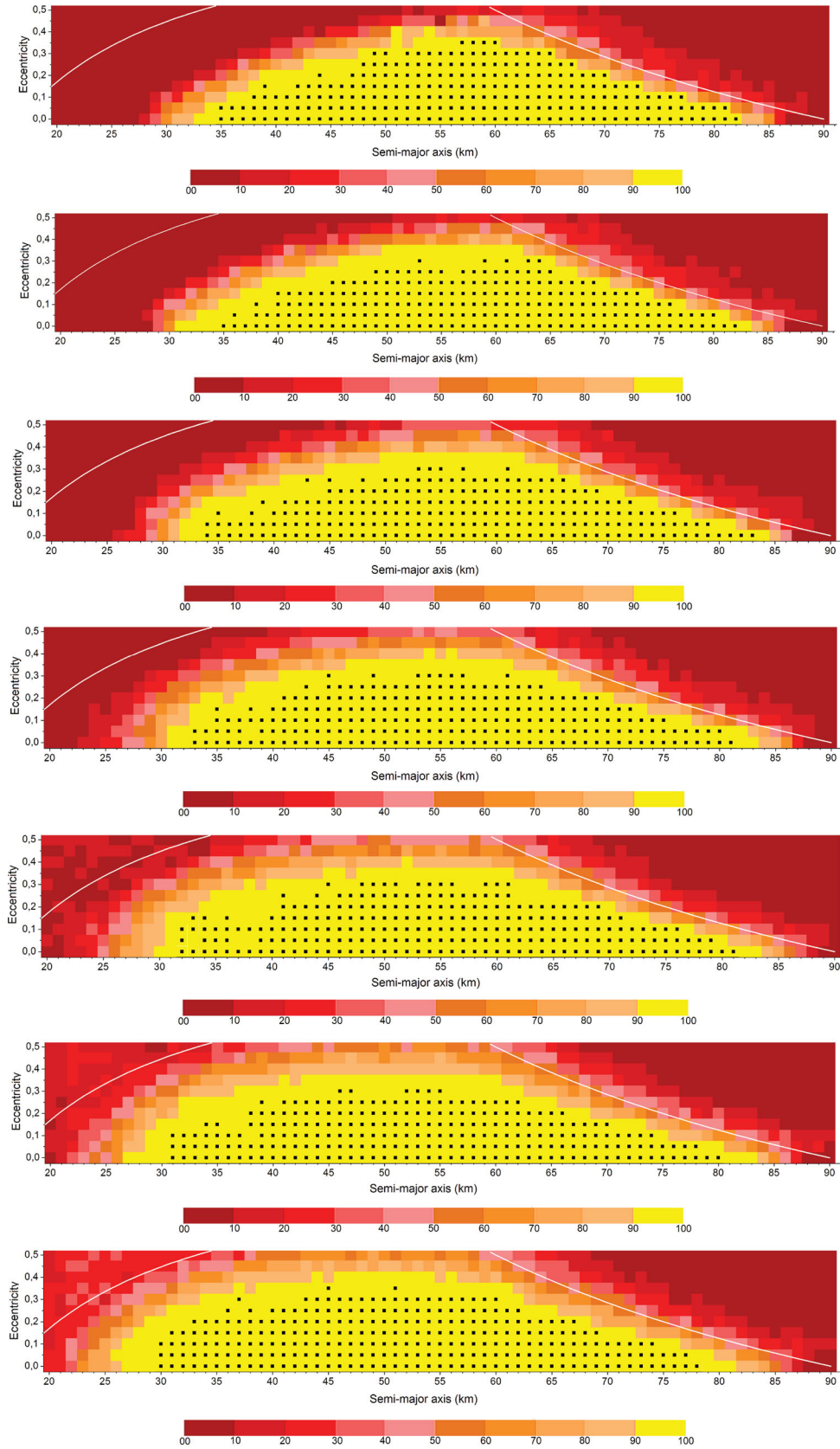


Figure 12. Diagram of stability of the external region for a time-span of 2 yr for $I = 0^\circ, I = 15^\circ, I = 30^\circ, I = 45^\circ, I = 60^\circ, I = 75^\circ$ and $I = 90^\circ$, from top to bottom. The white lines indicate the limits of the region. The yellow boxes marked with small black squares indicate the cases of 100 per cent survival.

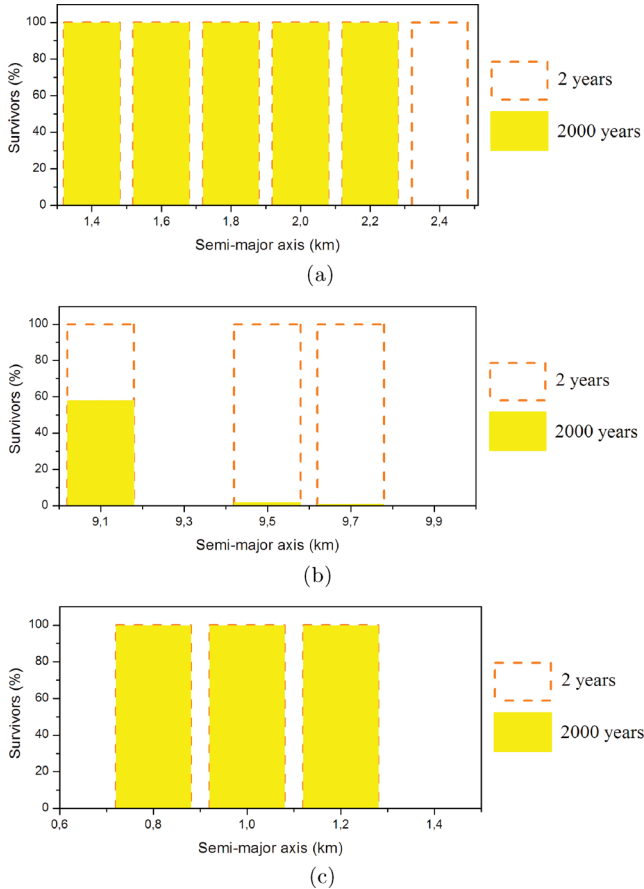


Figure 13. Percentage of survivors for each semi-major axis from (a) region 1, (b) region 2, and (c) region 3, corresponding to a stable region, for the planar and circular case. The dashed orange lines indicate the percentage of survivors for a time-span of 2 yr. The filled yellow columns indicate the percentage of survivors for a time-span of 2000 yr.

semi-major axis from regions 1, 2 and 3. The results are discussed separately.

(i) Region 1

In region 1, the set of particles with $e = 0.0$ and $I = 0^\circ$ that are stable for 2 yr are those with the semi-major axis ranging from 1.4 to 2.4 km (see the stability diagram in Fig. 2). From Fig. 13(a), we see that the region of stability for 2000 yr remains almost the same as that for 2 yr. Only the most external particles, with $a = 2.4$ km, were removed (100 per cent of collisions within 592 yr).

(ii) Region 2

For region 2, only three specific cases resulted in stability (i.e. 100 per cent survival in 2 yr) for the planar and circular case (see the stability diagram in Fig. 4). The long-term integrations show that these stable cases no longer survive for 2000 yr. From Fig. 13(b) it can be seen that the region of stability previously found for 2 yr in region 2 vanishes for the long period. In total, 48 per cent of the particles with $a = 9.1$ km are ejected from the system within 115 yr, while just 52 per cent of them survive for 2000 yr. For particles with $a = 9.3$ or 9.5 km 85 per cent of particles were ejected and 15 per cent experienced collisions, and therefore no particles survived for 2000 yr.

(iii) Region 3

In region 3, the set of particles with $e = 0.0$ and $I = 0^\circ$ stable for 2 yr are those with semi-major axis ranging from 0.8 to 1.2 km (see the stability diagram in Fig. 5). For region 3 we show that the

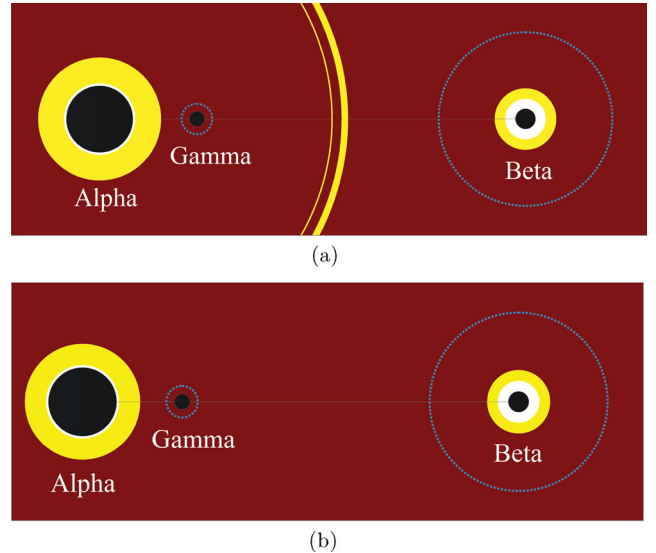


Figure 14. Representation of the stable (yellow) and unstable (red) regions in the internal region of the triple system 2001 SN263, considering the planar and circular case. (a) Short-term stability (period of 2 yr). (b) Long-term stability (period of 2000 yr).

region of stability for 2000 yr remains the same as that found for 2 yr (no collisions or ejections), as can be seen in Fig. 13(c).

The regions of stability found for short and long periods can be better visualized in the diagrams presented in Fig. 14, where only the special case treated in the present section is considered, that is, particles with circular and planar orbits in the internal regions of the triple system.

Both diagrams clearly show that the stable regions are very close to Alpha and Beta. For the short period (Fig. 14a) we have the small stable region in region 2 (region between Gamma and Beta) that vanishes for the long period (Fig. 14b). That was the most significant observable change between the short- and long-period cases. In addition, there is a smooth decrease of the stability region in region 1 (the region between Alpha and Gamma).

The results show that the system has a quick dispersion of particles; that is, the observable unstable region for 2 yr is almost the same as that for 2000 yr.

The long-term stable regions (yellow region in Fig. 14b) are an indication of regions where satellites or debris could be found within the system. In contrast, the short-term unstable regions (red region in Fig. 14a) are indicative of regions where such bodies would not be found.

9 FINAL COMMENTS

In this paper, we characterized the internal and external regions of stability and instability for the triple system of asteroid 2001 SN263, for a time-span of 2 yr. The region around the system was divided into four distinct regions (three of them internal to the system and one external). We performed numerical integrations of systems composed of seven bodies, namely the Sun, Earth, Mars, Jupiter and the three components of the system, and of thousands of particles randomly distributed within the demarcated regions, for the planar and inclined prograde cases.

For the planar case, it was shown that in the internal region the stable regions are very close to Alpha (region 1) and Beta (region 3). In the region between Beta and Gamma, here called region 2, we

showed that the particles experience the effects of resonances with Beta and Gamma. We identified that the particles in region 2 with $a \approx 8.0$ km are in a 3:1 resonance with Beta, and that particles with $a \approx 7.9$ km, in the same region, are in a 1:3 resonance with Gamma. The presence of such resonances and the presence of Beta and Gamma surrounding the region make region 2 an unstable region. Stability in region 2 was found only for some specific values of the initial semi-major axis ($a = 9.1, 9.5, 9.7$ km), and with an initial eccentricity $e = 0.0$.

We also analysed the inclined prograde case for the internal regions. Particles were considered with inclination relative to the equator of the central body in the interval $15^\circ \leq I \leq 90^\circ$, taken every 15° . For regions 2 and 3 we found that, until an inclination of $I = 30^\circ$ for region 2, and an inclination of $I = 45^\circ$ for region 3, the stable regions are similar to the regions found for the planar case. For inclinations higher than $I = 45^\circ$, the stable regions vanish. With such inclinations, the particles exceed the Kozai critical angle given by $I_{\text{crit}} \approx 39.2^\circ$. A known effect of the Kozai mechanism is the generation of oscillations of the eccentricity and of the mutual inclinations. These oscillations increase the probability of close encounters and collisions, and lead to the observed instability. The effects of the Kozai mechanism are also observable in region 1. The stable region decreases significantly for particles with $I \geq 60^\circ$ (except for $I = 90^\circ$, when there is a slight increase of the stable region). The results for region 1 also show that, with increasing inclination, the effect of the resonant motion between the particles and Gamma becomes observable. We found that the particles in this region with $a \approx 1.8$ km are in a 3:1 resonance with Gamma.

For the external region we found that the stable region is predominant. It was shown that the instability is found only in the neighbourhood of the limits of the region, namely in the vicinity of asteroid Beta (high collision probability) and beyond the border of the ejection-line. Inside those limits we found a significant stable region, where a large number of particles survive for 2 yr. The analysis of the inclined prograde cases for the external region shows that this region is not affected by the variation of inclination of the particles.

We also performed an analysis of the long-period stability for the internal regions, considering the planar and circular case, in order to capture the secular perturbations of the system. We found that the stable region found in region 1 for a period of 2 yr decreased slightly over 2000 yr. Only the most external particles were completely removed, in 592 yr. The stable regions found in region 2 for the 2-year period disappeared in the long period. The stability found in region 3 for 2 yr does not change over 2000 yr. Therefore, we see that the triple system 2001 SN263 has a quick scattering of particles; that is, most collisions and ejections happen in the early years.

The stable regions found for 2000 yr are an indication of where satellites or debris could be located in the system. Although the time-scale of 2000 yr is not sufficient to guarantee that, our results restrict the area to be considered in future research in this direction, and will guide the space mission in the search for such bodies. In contrast, we found that the unstable regions occur mostly in a short period of time (2 yr), so these regions are least likely to contain debris. Thus, thinking of the space mission, this is a good region to investigate in order to find sets of initial conditions that are unstable after 2 yr but that are stable over a shorter time-span that is long enough to accomplish the mission.

According to Fang & Margot (2011), the J_2 coefficient for Alpha is not a well-constrained value ($J_2 = 0.013 \pm 0.008$), and the present work shows that this coefficient plays an important role in

the dynamics of the system. A change in the J_2 value is expected to modify the dynamics, such as the resonance locations and the effects of the Kozai mechanism for the inclined cases. A study of the stable and unstable regions as a function of the J_2 coefficient demands a substantial effort in terms of new simulations and analysis, and is thus the subject of a future work.

ACKNOWLEDGMENTS

This work was funded by INCT – Estudos do Espaço, CNPq and FAPESP. This support is gratefully acknowledged. We thank Ernesto Vieira Neto for his help with the numerical integrator. The authors are also grateful to an anonymous referee for all their suggestions.

REFERENCES

- Amata G. B., 2009, Marco Polo Mission – Executive Summary. Thales Alenia Space, Spain, p. 15
- Anders E., 1964, *Space Sci. Rev.*, 3, 574
- D'arrigo P., 2003, The ISHTAR Mission Executive Summary for Publication on ESA Web Pages. Technical report. European Space Agency, Madrid
- Becker T., Howell E. S., Nolan M. C., Magri C., 2009, *BAAS*, 40, 437
- Bottke W., Melosh H. J., 1996, *Icarus*, 124, 372
- Brozovic M. et al., 2009, (136617) 1994 CC. *IAU Circ.*, 9053, 2
- Delsate N., Robutel P., Lemaître A., Carletti T., 2010, *Celest. Mech. Dyn. Astron.*, 108, 275
- Domingos R. C., Winter O. C., Yokoyama T., 2006, *MNRAS*, 373, 1227
- Everhart E., 1985, in Carusi A., Valsecchi G. B., eds, *Dynamics of Comets: Their Origin and Evolution*. Reidel, Holanda, p. 185
- Fang J., Margot J.-L., 2011, *AJ*, 141, 154
- Fang J., Margot J.-L., 2012, *AJ*, 143, 25
- Galvez A. et al., 2003, Near Earth Objects Space Mission Preparation: Don Quijote Mission Executive Summary. Technical report. European Space Agency, Madrid.
- Gladman B., Michel P., Froeschlé C., 2000, *Icarus*, 146, 176
- Kozai Y., 1962, *AJ*, 67, 591
- Marchis F., Descamps D., Hestroffer D., Berthier J., 2005, *Nat*, 436, 822
- Margot J. L., Nolan M. C., Benner L. A. M., Ostro S. J., Jurgens R. F., Giorgini J. D., Slade M. A., Campbell D. B., 2002, *Sci*, 296, 1445
- Morbidelli A., Bottke W. F., Froeschlé C., Michel P., 2002, *Origin and Evolution of Near-Earth Objects. Asteroids III*. Univ. Arizona Press, Tucson p. 409
- Murray D. C., Dermott S. F., 1999, *Solar System Dynamics*. Cambridge Univ. Press, Cambridge
- Nolan M. C., Howell E. S., Becker T., Magri C., Giorgini D., Margot J. L., 2008, in *Asteroids, Comets, Meteors*, paper no. 8258
- Opik E. J., 1961, *AJ*, 66, 381
- Pravec P. et al., 2006, *Icarus*, 181, 63
- Roy A. E., 1988, *Orbital Motion*, 3rd edn. IoP Publishing, Bristol
- Sears D. W. G., Scheeres D. J., Binzel R. P., 2004, *Adv. Space Res.*, 34, 2270
- Sukhanov A. A., Velho H. F. C., Macau E. E., Winter O. C., 2010, *Cosmic Res.*, 48, 443
- Wells N., 2003, SIMONE NEO Mission Study Executive Summary. Technical report. European Space Agency, Hampshire
- Winter O. C., Boldrin L. A. G., Vieira Neto E., Vieira Martins R., Giuliatti Winter S. M., Gomes R. S., Marchis F., Descamps P., 2009, *MNRAS*, 395, 218
- Yoshikawa M. et al., 2006, in *Workshop on Spacecraft Reconnaissance of Asteroid and Comet Interiors*, paper no. 3038

This paper has been typeset from a $\text{\TeX}/\text{\LaTeX}$ file prepared by the author.